**Late Holocene isotope hydrology of Lake Qinghai, NE Tibetan Plateau: effective moisture variability and atmospheric circulation changes**

Andrew C. G. Henderson[1, 2], Jonathan A. Holmes[2], and Melanie J. Leng[3, 4].

1. Department of Geographical & Earth Sciences, University of Glasgow, East Quadrangle, University Avenue, Glasgow, G12 8EU, UK;
2. Environmental Change Research Centre, University College London, Pearson Building, Gower Street, London, WC1E 6BT, UK;
3. NERC Isotope Geosciences Laboratory, British Geological Survey, Keyworth, Nottingham, NG12 5GG, UK;
4. School of Geography, University of Nottingham, Nottingham, NG7 2RD, UK.

**Abstract**

A sub-centennial-resolution record of lacustrine carbonate oxygen isotopes ($\delta^{18}O_C$) from the closed-basin Lake Qinghai on the NE Tibetan Plateau shows pronounced variability over the past 1500 years. Changes in $\delta^{18}O_C$ in hydrologically closed lakes are often interpreted in terms of changing effective moisture. Under this interpretation our record would imply increasing effective moisture during the Little Ice Age (LIA) compared to the Medieval Warm Period (MWP). However, independent evidence from other archives strongly suggests the Asian summer monsoon was stronger during the MWP and weakened during the LIA. Controls other than effective precipitation must therefore have contributed to the $\delta^{18}O_C$ values. We propose the LIA signal in Lake Qinghai resulted from a reduction in evaporation caused by colder air temperatures, coupled with a decrease in oxygen isotope composition of input waters as a result of an increase in the relative importance of westerly-derived precipitation. Our results caution against simplistic interpretations of carbonate oxygen isotope records from hydrologically-closed lakes and suggest all possible controlling factors must be taken into account in order to avoid misleading palaeoclimatic reconstructions.

**Keywords:** Lake Qinghai, oxygen isotope, Asian monsoon, Tibetan Plateau, late Holocene.

## 1. Introduction

Changes in the hydrological cycle and monsoon circulation are among the most serious of projected consequences of anthropogenically-induced warming for human society. Nowhere is this more acute than in Asia, where monsoon extremes can impact around half the world's population through drought or flooding. The thermal contrast between the Tibetan Plateau and the Indian and Pacific Oceans drives the most convectively active atmospheric circulation system on Earth and produces the seasonal monsoon rains (Webster et al., 1998). Several studies (Meehl & Arblaster, 2003; Shindell et al., 2006; Stowasser et al., 2009) suggest continued warming will increase mean annual precipitation, but also create greater inter-annual monsoon variability.

Palaeoclimate records show the monsoon has gradually weakened over the Holocene as a whole in a response to reduced orbital forcing, while hydrological changes at the decadal to millennial timescale appear to correlate with North Atlantic cold phases (Porter & Zhou, 2006; Wang et al., 2005). The modeled future response of the tropical hydrological cycle to projected greenhouse gas increases is similar to these past changes (Shindell et al., 2006). However, there is a paucity of long-term metereological data sets from this region and in order to predict future changes in monsoon rains, an understanding of the natural variability of climate beyond the short observational record is needed. We therefore depend on proxy climate records, which offer valuable insight into the mechanisms underlying potential future climate change in Asia.

The Little Ice Age (LIA) is the most widely documented recent cold phase in the North Atlantic region. It was preceded by the more ambiguously identified Medieval Warm

Period (MWP). The LIA and MWP are the two most distinct climate anomalies of the past *c.* 1500 years. However, our knowledge of monsoon variability during these anomalies is limited. Palaeoclimate records from low latitude sites show a strengthening of the monsoon over the past few centuries (e.g. Anderson et al., 2002; Wang et al., 2005). In contrast, the few proxy records available from the region of the monsoon-limit show no clear overall trend in climate during this time (Thompson et al., 2003; Yang et al., 2003). Furthermore, recent observations from the Tibetan Plateau document a 1.8°C rise in temperature over the last 50 years that is concurrent with an increase in precipitation across East Asia (Wang et al., 2008).

High-resolution late Holocene proxy records from the climatically sensitive region of the monsoon are clearly required to identify the spatial and temporal patterns of monsoon variability. Here we present a sub-centennial-scale oxygen isotope record from lake sediment carbonates ($\delta^{18}O_C$), spanning the LIA and MWP, from Lake Qinghai in China. Lake Qinghai is located in a region dominated by atmospheric circulation that is influenced by the Asian summer monsoon, westerly jet stream and Siberian high. It currently lies close to the limit of the modern Asian summer monsoon, so this location should be sensitive to temporal shifts in the monsoon boundary.

## 2. Study Site

Lake Qinghai (37°N, 100°E, 3192 m a.s.l, surface area = 4400 $km^2$, max. depth = 27 m) lies in an intermontane depression on the northeastern corner of the Tibetan Plateau (Fig. 1). It has no visible surface outflows and the excess of evaporation (*c.* 1000 mm $a^{-1}$) over precipitation (*c.* 400 mm $a^{-1}$) has produced a brackish/saline alkaline lake (salinity

= 14.5 g $l^{-1}$, pH = 9.15 – 9.30) (LZCAS, 1994). Temperature around the Lake Qinghai region varies between 10.4 and 15.2°C in July and between –10.4 and –14.7°C in January, with a mean annual value of – 0.7°C.

## 3. Material and methods

A 78 cm sediment core (QING6) was recovered from the deepest part of the southern basin (Fig. 1) using a mini-Mackereth piston corer in May 1999. It was sampled contiguously at 0.5 cm for the upper 30 cm and at 1 cm for the lower 48 cm, in the field. The oxygen isotope composition of authigenic carbonate was measured using a vacuum extraction technique and a VG Optima dual-inlet mass spectrometer with an analytical precision <0.1‰ ($\delta^{13}C$ not reported here). Modern waters were collected in May and October 2001 and $\delta^{18}O$ and δD were determined using $CO_2$ equilibration and by zinc reduction respectively, before dual-inlet mass spectrometry using a VG IsoGas Sira.

## 4. Chronology

The chronology for QING6 is based on $^{210}Pb$, $^{137}Cs$ and 3 AMS $^{14}C$ dates on bulk organic carbon as terrestrial macrofossils are very rare in the lake sediments. The AMS $^{14}C$ ages have been corrected for an old carbon error (OCE) that has previously been documented in Lake Qinghai (e.g. Shen et al., 2005; Yu et al., 2007) and we define a new OCE that represents the best estimate for Lake Qinghai to date. Discussion of the development of this chronological framework is below.

### 4.1 $^{210}Pb$ dating

The $^{210}$Pb chronology was determined using a proxy method, which measured $^{210}$Pb activity through its granddaughter product $^{210}$Po at 10 intervals within the top 30 cm of core QING6. The method employed is based on Flynn (1968) and used double acid leaching of between 1.5 and 2 grams of dry sediments with $^{209}$Po as an isotopic tracer. This was followed by autodeposition of the Po isotopes in the leachate on to silver discs. These were counted for a minimum of 400000 seconds, and detection limits were 0.1 Bq/kg. Unsupported $^{210}$Pb activity was calculated by subtraction of the supported activity (calculated by $^{210}$Pb activity at depth in the core) from the total activity at each level (Table 1). Dates were determined according to the constant sedimentation rate model (log-linear straight line fit) (Fig. 2).

### 4.2 $^{137}$Cs dating

Age models based on $^{210}$Pb activity are often corroborated using $^{137}$Cs, an artificial radionuclide, which is present in the environment due to nuclear weapons testing and nuclear reactor accidents. Global release began in 1952, with peak input into the environment in 1958/59 and 1963 (due to pre-treaty increases in above-ground nuclear testing), 1971 (southern hemisphere) and 1986 (in some regions that were impacted by Chernobyl). $^{137}$Cs in QING6 shows considerable amount of penetration down core below its peak at 1.5 cm (to a depth of ~6 cm) (Table 2, Fig. 2) and estimates an accumulation rate of 0.42 mm/yr. This is rather conservative compared to the $^{210}$Pb inferred accumulation rates.

### 4.3 $^{14}$C dating

AMS $^{14}C$ ages were determined on bulk organic matter in the absence of terrestrial macrofossils (Table 3). Each date was corrected by an old carbon error of 658 years determined for Lake Qinghai based on modern observations (see discussion below). These dates were then calibrated using OxCal v. 4.0 (Bronk Ramsey, 1995, 2001) using the IntCal04 calibration curve (Reimer et al., 2004) (Table 3).

### 4.4 Old carbon error

Establishing reliable age models for Lake Qinghai is hampered by the existence of an old carbon error (OCE). The introduction of 'old' carbon from the catchment into the lake gives an apparent age to the carbon pool (Table 4), which is then transferred to any aquatic plants in the lake, giving rise to a radiocarbon age older than expected. Previous studies have attempted to quantify this OCE for Lake Qinghai (e.g. Shen et al., 2005; Yu et al., 2007) via a number of different approaches.

Shen et al. (2005) proposed an offset of 1039 years based on a linear regression between 10 AMS $^{14}C$ dates of total organic carbon spanning the late Pleistocene/Holocene period. The dates were subsequently corrected by this offset and an age model established by linear interpolation. The authors assume there are uniform sedimentation and that the OCE remained constant through time. Unfortunately, there is no $^{210}Pb$ and/or $^{137}Cs$ dating to independently verify this age model in the upper sediments of their core.

Yu et al. (2007) present a two-box model, based on radiocarbon mass balance in lake water and in the early diagenetic zone, which suggests that the OCE is 1500 years. The model suggests that the OCE is a result of 'old' carbon being introduced into the lake via riverine and/or groundwater inputs. Because the flux of this 'old' carbon is controlled by its concentration in the input water and the lake's hydrological state, the OCE is unlikely to have remained constant over the entire late Pleistocene/Holocene. In particular, the degree of exchange of carbon with atmospheric $CO_2$ will vary with the lake's residence time, as residence time increases or decreases, leading to an increase and decrease, respectively, in age of the lake's DIC. Moreover, the OCE estimate of 1500 years, if applied to the AMS $^{14}C$ ages for QING6 would yield post-bomb ages for all of our radiocarbon dates, which clearly cannot be reconciled with the $^{210}Pb$- and $^{137}Cs$-inferred age models.

We have established an independent OCE for Lake Qinghai using two approaches. Firstly, we measure the $^{14}C$ of dissolved organic carbon (DOC) in modern lake water, surface sediment bulk organic carbon (BO) and surface sediment authigenic carbonate (AC) (Table 4). Combination of these dates using OxCal v. 4.0 (Bronk Ramsey, 1995, 2001), gives a median calendar age for the 'modern' environment of 658 cal. yrs BP ±19. This is significantly younger than other estimates of the OCE by Shen et al. (2005) and Yu et al. (2007). Secondly, we apply by the same approach as Shen et al., (2005) by fitting a linear regression through the uncalibrated radiocarbon ages for QING6 (Fig. 3). This is done to determine the intercept of the curve on the age axis of the age-depth plot. This procedure provides an estimated OCE of ~737 years BP, which is very similar to the value derived from modern observations. This suggests (1) we can use the modern radiocarbon observations to correct our AMS $^{14}C$ data, and (2) the OCE appears to have been relatively constant throughout the last 1500 years.

## 4.4 Age model

A mixed-effect regression model (Heegaard et al., 2005) was fitted through the calibrated median range of our AMS $^{14}C$ ages (Table 3), the lowest $^{210}Pb$-inferred age (Table 1) and the surface of the sediment core. This procedure has advantages over others, in that it allows the inclusion of all age determinations and any specific *a priori* information e.g. surface sediment = modern day. It uses the central point (in this case the median calibrated age) and a measurement of the within-object uncertainty. The model then examines between-object variability in the context of the magnitude of the within- and between-error of a single dated object. If the variability between two radiocarbon ages is large in comparison with the distribution of the calibrated variability it can be identified as an outlier (see Heegaard et al., 2005 for more information). In the case of QING6, the AMS $^{14}C$ age at 61 – 62 cm (852, 1σ = 798 – 871) is statistically identified as an outlier by a Markov Chain Monte Carlo algorithm (see Bronk Ramsey, 2008) and there is little overlap between the *posterior* probability distribution and the *likelihood* probability distribution of the date at 61 – 62 cm with the other calibrated ages. This overlap is calculated in the form of an *agreement index* (Bronk Ramsey, 1995) and gives the likelihood of the posterior model to that of a 'null' model (Bronk Ramsey, 2008). The AMS $^{14}C$ age at 61 – 62 cm has a low agreement index (17%), which is below the *good agreement* threshold set at > 60%.

Based on the poor agreement of the radiocarbon age at 61 – 62 cm, we exclude it in the development of our age model for QING6, although we have modelled it for comparison (Fig. 4). A generalized additive model with a quasi-likelihood distribution (Heegaard et al., 2005) was used to generate the regressions for the age model and provides a robust fit to our individual age determinations (Fig. 4).

## 5. Results

The QING6 record has a $\delta^{18}O_C$ range of ~2.2‰ (Fig. 5B) and exhibits a series of sub-centennial (2000 to 1000 AD) and centennial (1000 to 500 AD) fluctuations broadly similar to those documented in Northern Hemisphere temperature reconstructions (Moberg et al., 2005), which themselves strongly resonate with a China-wide temperature-anomaly record (Yang et al., 2002) (Fig. 5C). One of the most pronounced features of the isotope record is the abrupt negative shift of ~1.7‰ centered at *c.* 1400 AD (Fig. 5B), which is followed by rapid changes of up to 1.5‰ around a mean value of 0.5‰, in contrast to a more positive mean of ~1.3‰ with fluctuations of only 0.5‰. This shift in $\delta^{18}O_C$ values potentially represents a significant change in Lake Qinghai's isotope hydrology. Another key feature of the late Holocene record is the prominent, ~2‰ shift to more negative $\delta^{18}O_C$ within the last 200 years, culminating in the most negative $\delta^{18}O_C$ for the whole record at 1950 AD (Fig. 5B). Subsequently, $\delta^{18}O_C$ increased up to the present day to a value of ~1.3‰.

## 6. Lake Qinghai isotope palaeohydrology

The $\delta^{18}O$ of lacustrine authigenic carbonate ($\delta^{18}O_C$) is controlled by the $\delta^{18}O$ of lake water ($\delta^{18}O_{LW}$), water temperature, and carbonate mineralogy. $\delta^{18}O_{LW}$ is, in turn, controlled by the isotopic composition of input water, which is dependent on the condensation temperature and moisture-source history of precipitation ($\delta^{18}O_P$), as well as evaporative flux from the lake's surface. In hydrologically closed lakes, such as Lake

Qinghai, changes in water volume (and lake level), chemistry and $\delta^{18}O_{LW}$ commonly result from variations in effective moisture: the balance of inputs (precipitation) over outputs (evaporation) (P/E; Leng & Marshall, 2004). When P/E decreases, the lake water becomes enriched with $^{18}O$ because of the preferential evaporative loss of water $^{16}O$, whereas the opposite occurs during periods of increased effective moisture.

Change in temperature-dependent $^{18}O$ fractionation from lake water into carbonate is unlikely to have been the main control on $\delta^{18}O_{C}$, because a 1°C temperature change would have caused a shift in $\delta^{18}O_{C}$ of only about 0.24‰, all other things being equal (Hays & Grossman, 1991). If water temperature were solely responsible for changes in $\delta^{18}O_{C}$ then the abrupt 1.7‰ fall in $\delta^{18}O_{C}$ at *c.* 1400 AD (Fig. 5B) would have required a temperature increase of ~6°C, which is untenable. Carbonates in QING6 comprise solely calcite, confirming that mineralogical variations cannot explain changes in $\delta^{18}O_{C}$ either. The major influence on $\delta^{18}O_{C}$ must therefore be the isotopic composition of lake water ($\delta^{18}O_{LW}$), which in turn is determined by the oxygen isotope composition of input water ($\delta^{18}O_{I}$) and the balance of precipitation to evaporative enrichment (P/E).

Lake Qinghai is fed by direct precipitation and by catchment runoff mainly via large rivers. The average $\delta^{18}O$ of large rivers on the Tibetan Plateau is close to the weighted mean annual $\delta^{18}O_{P}$ (Hren et al., 2009) and therefore, $\delta^{18}O_{I}$ is mainly influenced by the composition of regional precipitation. The rivers flowing into Lake Qinghai had $\delta^{18}O$ values between –5.9 and –7.7‰ (Fig. 6) in May 2000 and the modern $\delta^{18}O_{LW}$ of the lake is + 2.7‰. $\delta^{18}O_{LW}$ is therefore $^{18}O$-enriched compared to $\delta^{18}O_{I}$ (Fig. 6), confirming the lake water has undergone evaporative enrichment. Also, the water history of the lake level and coeval $\delta^{18}O_C$ variations is correlated over the last ~50 years (Henderson et al., 2003). Because lake level is controlled by effective moisture, $\delta^{18}O_C$ would be expected to be a good proxy for P/E.

If the $\delta^{18}O_C$ record were indeed a proxy for effective moisture, then the climatic interpretation would reflect variability in the intensity of the Asian summer monsoon. Using this model, the positive $\delta^{18}O_C$ values between 500 and 1000 AD would imply a weaker monsoon that subsequently became stronger during the MWP between 1050 and 1250 AD (Fig. 5B). In the same way, the marked step-wise shift to lower $\delta^{18}O_C$ values at *c.* 1400 AD suggests a further strengthening of the Asian summer monsoon during the LIA (Fig. 5B). The oscillations between 1850 AD and present would imply a weakening of the monsoon until *c.* 1900 AD followed by greater monsoon intensity, as inferred by the lowest $\delta^{18}O_C$ values in the entire record at 1950 AD. Since 1950 AD, our record suggests a trend to decreasing effective moisture that would imply a weakening in the Asian summer monsoon circulation (Fig. 5B).

## 7. Discussion

Regional palaeoclimatic archives (Fig. 5B-E) indicate an abrupt change in climate around 1400 AD that coincides with the change in $\delta^{18}O_c$ in QING6. This change includes an abrupt cooling associated with the LIA (Fig. 5C), the start of a prolonged drought (Tan et al., 2008) (Fig. 5D) and a weakening of the Asian summer monsoon (Zhang et al., 2008) (Fig. 5E). In particular, Zhang et al. (2008) highlight (1) a strong monsoon during the MWP, which is similar to the small shift to more negative $\delta^{18}O_C$ values between 1100 and 1250 AD in Lake Qinghai; and (2) a weak monsoon during the LIA, which is in disagreement with a "classical" interpretation of the QING6 $\delta^{18}O_C$ record in terms of P/E. The speleothem record also shows a weakening of the Asian summer monsoon during the last 50 years of the 20$^{th}$ Century however, which is consistent with the trend to more positive $\delta^{18}O_c$ values in our record (Fig. 5B). A drought/flood (D/F) index proposed by Tan et al. (2008) indicates more arid conditions and decreased monsoon intensity during the LIA (Fig. 5). The MWP occurred during a period of strengthened summer monsoon (Fig. 5E), implicating increased precipitation over the region as a major control on $\delta^{18}O_C$ in QING6 (Fig. 5D), while the last 50 years of the 20$^{th}$ Century saw a reduction in monsoon strength and $\delta^{18}O_C$ responded accordingly.

Liu et al. (2009) show that during the late Holocene an intensified Asian winter monsoon correlated with cold events in the North Atlantic and a significant shift in climate between the MWP and LIA was mediated by an enhanced westerly jet stream. Yu et al. (2008a) also propose there has been a gradual decay in the strength of the Asian summer monsoon system over the last 2000 years, with a step-wise shift to a weakened monsoon state during the LIA over the northern Tibetan Plateau. A multi-proxy ice core record from Mt. Everest provides evidence for such synoptic changes in climate during the LIA (Kaspari et al., 2007). It implies large decreases in marine air mass incursions (linked to the Asian summer monsoon) and an overall increase in incursions of continental air masses (linked to the westerly jet stream), supporting a climate scenario of a weakening monsoon influence from the beginning of the LIA in southern Tibet. Kaspari et al. (2007) propose that these shifts are associated with relatively high pressures over the continental interior during the summer monsoon season and consequently a reduction in the northward extension of the Asian summer monsoon. All of these changes occurred at a similar time to the prominent 1.7‰ negative shift in $\delta^{18}O_C$ in Lake Qinghai, which suggests climate during the LIA is possibly controlled, at least in part, by the westerly jet stream.

Most palaeoclimatic archives support the interpretation of low $\delta^{18}O_C$ values in QING6 as indicative of wet conditions during the MWP. However, during the LIA the Lake Qinghai $\delta^{18}O_C$ record conflicts with all the other proxy records, implying these factors other than effective precipitation must be important in controlling $\delta^{18}O_C$. These other factors could be (1) a change in the $\delta^{18}O_P$ of regional precipitation, which will affect $\delta^{18}O_I$; (2) reduction in evaporation as a result of decrease in temperature, which would reduce the loss of $H_2{}^{16}O$ to the atmosphere, thereby causing less $^{18}O$ enrichment of lake water, and so effectively lowering $\delta^{18}O_{LW}$ or (3) a combination of both.

Changes in evaporative flux from lake-surface waters and in the isotopic composition of inflow are both potentially important controls of the $\delta^{18}O_{LW}$ of Lake Qinghai. Colder air temperatures during the LIA could have reduced evaporative flux and hence $^{18}O$ enrichment of lake water and in turn, authigenic carbonates forming in the lake. However, an alkenone record from the north basin of Lake Qinghai suggests positive covariance between temperature and salinity over the past 3000 years, implying that cold intervals such as the LIA were accompanied by a more arid climate. This would preclude an interpretation of the QING6 $\delta^{18}O_C$ record in terms of increased effective moisture during the LIA. Furthermore, reduced temperatures during the LIA would counteract the effect of evaporation on $\delta^{18}O_{LW}$ because colder water causes greater $^{18}O$

enrichment in carbonate because of the temperature-dependent $^{18}O$ fractionation from lake water into carbonate (Hays & Grossman, 1991).

If a reduction in evaporative flux from Lake Qinghai cannot by itself explain the reduction in $\delta^{18}O_C$ during the LIA, some other mechanism must be sought (e.g. Holmes et al., 2007). As discussed above, the isotopic composition of Lake Qinghai water is sensitive to changes in the composition of precipitation input. At present, the $\delta^{18}O_P$ is strongly correlated with air temperature and shows little amount effect associated with the Asian summer monsoon (Araguás-Araguás et al., 1998; Johnson & Ingram, 2004; Tian et al., 2007; Yu et al., 2008b). Over a long period, however, $\delta^{18}O_P$ may also be controlled changes in the relative importance of different air masses bringing moisture to the NE Tibetan Plateau, in particular, from monsoonal versus westerly sources. Modern observations of $\delta^{18}O_P$ over the Tibetan Plateau confirm that moisture from a westerly source is more $^{18}O$-depleted than that associated with the summer monsoon (Tian et al., 2007), owing to greater 'rain-out' as the air passes over central Asia.

Given the wealth of evidence for cold and dry conditions over the Tibetan Plateau during the LIA, reduced $\delta^{18}O_C$ values in QING6 during this interval seems best explained by a switch to a greater proportion of moisture from $^{18}O$-depleted westerly sources, coupled with reduced evaporative enrichment of the lake water caused by lower surface-water temperature. Conversely, during the MWP and also the mid-20$^{th}$ Century a strengthening of the summer monsoon would have led to the input of a greater proportion of precipitation that was less $^{18}O$-depleted than that associated with the westerlies. This would have countered the increased evaporative flux caused by higher water temperatures, leading to an increase in $\delta^{18}O_{LW}$ and hence $\delta^{18}O_C$.

The influence of the westerlies on Asian climate during the Holocene has been previously noted. Vandenberghe et al. (2006) suggest that during cold intervals, North Atlantic climate penetrates eastward via the westerly jet and during warm conditions the Asian summer monsoon effects are stronger and therefore counteract the influence of the westerlies. Porter and Zhou (2006) have also documented a close link between circulation over the North Atlantic and China. They showed that periods of enhanced loess deposition from a strengthened winter monsoon produced by colder, drier conditions are associated with ice-drift events in the North Atlantic, which represent episodic migrations of cold polar water southward into warmer sub-polar waters (Porter & Zhou, 2006).

Given the location of Lake Qinghai at the northern extent of the contemporary Asian summer monsoon precipitation boundary, a weakening of monsoon circulation would place the lake outside its influence. This appears to have occurred during the LIA as changes in our $\delta^{18}O_C$ record coincide with a weakening of the summer monsoon coupled with reduced effective moisture and lower air temperatures. These intervals of low $\delta^{18}O_C$ values in QING6 record suggest that the relative importance of the westerly jet stream in controlling climate over the NE Tibetan Plateau was greater during the LIA. This contrasts with the MWP and mid-20$^{th}$ Century, when the summer monsoon was stronger and effective moisture over the Lake Qinghai catchment increased. Previous studies have revealed similar types of change in the synoptic pattern of atmospheric circulation over the Tibetan Plateau during the past 1500 years (e.g. Kaspari et al., 2007; Liu et al., 2009; Yu et al., 2008a). In particular, Kaspari et al. (2007) suggest the Asian continental atmospheric system played a more active role in determining climate over the Tibetan Plateau and NW China during the LIA, while the Asian summer monsoon was more important during the MWP.

## 8. Conclusion

Multiple factors often preclude a simple interpretation of lake-sediment oxygen-isotope records as in the case of Lake Qinghai. By placing our $\delta^{18}O_C$ record in the context of regional palaeoenvironmental archives we have developed a model of climate history for the last 1500 years. If the classical interpretation of oxygen-isotopes for a semi-arid, hydrologically closed-basin is applied to Lake Qinghai it would provide a misleading palaeoclimatic reconstruction, especially for the LIA. Instead, we argue there are two main controls on $\delta^{18}O_C$ under two different climate scenarios: (1) in warmer conditions the Asian summer monsoon brings more precipitation to the NE Tibetan Plateau, and (2) under colder temperatures the westerly jet stream has greater influence on the climate in the region. We caution against simplistic interpretations of carbonate oxygen isotope records from lakes and suggest all possible controlling factors must be taken into account.

**Acknowledgements** We thank the Dudley Stamp Memorial Fund (The Royal Society), UCL Graduate School, UCL Department of Geography and Environmental Change Research Centre for funding the fieldwork. Stable isotope analyses were undertaken with a NERC Isotope Geosciences Laboratory allocation (IP/679/1100) and radiocarbon dates by a NERC-RCL allocation (RCL1004.1002), as well as additional dates provided by Tim Jull at the NSF-Arizona AMS Facility. We are grateful to Andy Cundy, University of Brighton, who provided his expertise on $^{210}Pb$ and $^{137}Cs$ dating. Invaluable logistical support was provided by the Center for Arid Environment and Paleoclimate (CAEP) research group at Lanzhou University, in particular, Fahu Chen and Jiawu Zhang. We also thank Tan Liancheng for the D/F Index.

## References

Anderson, D.M., Overpeck, J.T., Gupta, A.K., 2002. Increase in the Asian southwest monsoon during the past four centuries. Science 297, 596-599.

Araguás-Araguás, L., Froehlich, K., Rozanksi, K., 1998. Stable isotope composition of precipitation over southeast Asia. Journal of Geophysical Research-Atmospheres 103, D22, 28721-28742.

Hays, P.D., Grossman, E.L., 1991. Oxygen isotopes in meteoric calcite cements as indicators of continental palaeoclimate. Geology 19, 441-444.

Heegaard, E., Birks, H.J.B., Telford, R.J., 2005. Relationships between calibrated ages and depth in stratigraphical sequences: an estimation procedure by mixed-effect regression. Holocene 15, 612-618.

Henderson, A.C.G., Holmes, J.A., Zhang, J.W., Leng, M.J.,Carvalho, L.R., 2003, A carbon- and oxygen-isotope record of recent environmental change from Qinghai Lake, NE Tibetan Plateau. Chinese Science Bulletin 48, 1463-1468.

Holmes, J.A., Zhang, J.W., Chen, F.H., Qiang, M.R., 2007. Paleoclimatic implications of an 850-year oxygen-isotope record from the northern Tibetan Plateau. Geophysical Research Letters 34, L23403.

Hren, M.T., Bookhagen, B., Blisniuk, P.M., Booth, A.L., Chamberlain, C.P., 2009. $\delta^{18}O$ and $\delta D$ of streamwaters across the Himalaya and Tibetan Plateau: implications for moisture sources and paleoelevation reconstructions. Earth and Planetary Science Letters 288, 20-32.

Hua, Q., Barbetti, M., 2004. Review of tropospheric bomb C-14 data for carbon cycle modeling and age calibration purposes: Radiocarbon 46, 1273-1298.

Johnson, K.R., Ingram, B.L., 2004. Spatial and temporal variability in the stable isotope systematics of modern precipitation in China: implications for palaeoclimate reconstructions. Earth and Planetary Science Letters 220, 365-377.

Kaspari, S., Mayewski, P., Kang, S., Sneed, S., Hou, S., Hooke, R., Kreutz, K., Introne, D., Handley, M., Maasch, K., Qin, D., Ren, J., 2007. Reduction in northward incursions of the South Asian monsoon since ~1400 AD inferred from a Mt. Everest ice core. Geophysical Research Letters 34, L16701.

Leng, M.J., Marshall, J.D., 2004. Palaeoclimate interpretation of stable isotope data from lake sediment archives. Quaternary Science Reviews 23, 811-831.

Liu, X., Dong, H., Yang, X., Herzschuh, U., Zhang, E., Stuut, J-B.W., Wang, Y., 2009. Late Holocene forcing of the Asian winter and summer monsoon as evidenced by proxy records from the northern Qinghai-Tibetan Plateau. Earth and Planetary Science Letters 280, 276-284.

Liu, Z.H., Henderson, A.C.G., Huang, Y.S., 2006. Alkenone-based reconstruction of late-Holocene surface temperature and salinity in Lake Qinghai, China. Geophysical Research Letters 33, L09707.

LZCAS (Lanzhou Branch of Chinese Academy of Sciences), 1994. Evolution of recent environments in Qinghai Lake and its prediction. West Center of Resource and Environment, Chinese Academy of Sciences, Science Press, Beijing (in Chinese with English abstracts).

Meehl, G.A., Arblaster, J.M., 2003. Mechanisms for projected future changes in south Asian monsoon precipitation. Climate Dynamics 21, 659-675.

Moberg, A., Sonechkin, D.M., Holmgren, K., Datsenko, N.M., Karlen, W., 2005. Highly variable Northern Hemisphere temperatures reconstructed from low- and high-resolution proxy data. Nature 433, 613 – 617.

Porter, S.C., Zhou, W.J., 2006. Synchronism of Holocene East Asian monsoon variations and North Atlantic drift-ice tracers. Quaternary Research 65, 443-449.

Ramsey, C.B., 1995. Radiocarbon calibration and analysis of stratigraphy: The OxCal program: Radiocarbon 37, 425-430.

Ramsey, C.B., 2001. Development of the radiocarbon calibration program: Radiocarbon 43, 355-363.

Ramsey, C.B., 2008. Deposition models for chronological records. Quaternary Science Reviews 27, 42-60.

Reimer, P.J., Baillie, M.G.L., Bard, E., Bayliss, A., Beck, J.W., Bertrand, C.J.H., Blackwell, P.G., Buck, C.E., Burr, G.S., Cutler, K.B., Damon, P.E., Edwards, R.L., Fairbanks, R.G., Friedrich, M., Guilderson, T.P., Hogg, A.G., Hughen, K.A., Kromer, B., McCormac, G., Manning, S., Ramsey, C.B., Reimer, R.W., Remmele, S., Southon, J.R., Stuiver, M., Talamo, S., Taylor, F.W., van der Plicht, J., Weyhenmeyer, C.E., 2004. IntCal04 terrestrial radiocarbon age calibration, 0-26 cal kyr BP. Radiocarbon 46, 1029 – 1058.

Shen, J., Liu, X.Q., Wang, S., Matsumoto, R., 2005. Palaeoclimatic changes in the Qinghai Lake area during the last 18,000 years. Quaternary International 136, 131-140.

Shindell, D.T., Faluvegi, G., Miller, R.L., Schmidt, G.A., Hansen, J.E., Sun, S., 2006. Solar and anthropogenic forcing of tropical hydrology. Geophysical Research Letters 33, L24706.

Stowasser, M., Annamalai, H., Hafner, J., 2009. Response of the South Asian Summer Monsoon to Global Warming: Mean and Synoptic Systems. Journal of Climate 22, 1014-1036.

Tan, L.C., Cai, Y., Yi, L., An, Z.S., Ai, L., 2008. Precipitation variations of Longxi, northeast margin of Tibetan Plateau since AD 960 and their relationship with solar activity. Climate of the Past 4, 19-28.

Thompson, L.G., Mosley-Thompson, E., Davis, M.E., Lin, P.N., Henderson, K.A., Mashiotta, T.A., 2003. Tropical Glacier and Ice Core Evidence of Climate Change on Annual to Millennial Time Scales. Climatic Change 59, 137 – 155.

Tian, L., Yao, T.D., MacClune, K., White, J.W.C., Schilla, A., Vaughn, B., Vachon, R., Ichiyangi, K., 2007. Stable isotopic variations in west China: a consideration of moisture sources. Journal of Geophysical Research 112, D10112.

Vandenberghe, J., Renssen, H., von Huissteden, K., Nugteren, G., Konert, M., Lu, H., Dodonov, A., Buylaert, J-P., 2006. Penetration of Atlantic westerly winds into Central and East Asia. Quaternary Science Reviews 25, 2380-2389.

Wang, B., Bao, Q., Hoskins, B., Wu, G., Liu, Y., 2008. Tibetan Plateau warming and precipitation changes in East Asia. Geophysical Research Letters 35, L14702.

Wang, Y.J., Cheng, H., Edwards, R.L., He, Y., Kong, Z., An, Z.S., Wu, J., Kelly, M.J., Dykoski, C.A., Li, X., 2005. The Holocene Asian monsoon: Links to solar changes and North Atlantic climate. Science 308, 854 – 857.

Webster, P.J., Magana, V.O., Palmer, T.N., Shukla, J., Tomas, R.A., Yanai, M., Yasunari, T., 1998. Monsoons: Processes, predictability, and the prospects for prediction. Journal of Geophysical Research-Oceans 103, C7, 14451-14510.

Yang, B., Bräuning, A., Shi, Y.F., 2003. Late Holocene temperature fluctuations on the Tibetan Plateau. Quaternary Science Reviews 22, 2335-2344.

Yang, B., Bräuning, A., Johnson, K.R., Shi, Y.F., 2002. General characteristics of temperature variation in China during the last two millennia. Geophysical Research Letters 29, 1324.

Yu, S.Y., Ricketts, R.D., Colman, S.M., 2008a. Determining the spatial and temporal patterns of climate changes in China's western interior during the last 15ka from lacustrine oxygen isotope records. Journal of Quaternary Science 24, 237-247.

Yu, W., Yao, T., Tian, L., Ma, Y., Ichiyanagi, K., Yu, W., Sun, W., 2008b. Relationships between $\delta^{18}O$ in precipitation and air temperature and moisture origin on a south–north transect of the Tibetan Platea. Atmospheric Research 87, 158-169.

Yu, S.Y., Shen, J., Colman, S.M., 2007. Modeling the radiocarbon reservoir effect in lacustrine systems. Radiocarbon 49, 1241-1254.

Zhang, P.Z., Cheng, H., Edwards, R.L., Chen, F., Wang, Y.J., Yang, X., Liu, J., Tan, M., Wang, X.F., Liu, J.H., An, C., Dai, Z., Zhou, J., Zhang, D., Jia, J., Jin, L., Johnson, K.R., 2008. A test of climate, sun, and culture relationships from an 1810-year Chinese cave record. Science 322, 940-942.

**Table 1:** Summary of analyses used to determine $^{210}Pb$ chronology in QING6. Supported $^{210}Pb$ activity, determined at the base of the core was 0.025 Bq/g. Depths are midpoints of each interval.

| Depth (cm) | $^{210}Po$ Activity (Bq/g) | Unsupported $^{210}Pb$ (Bq/g) | Error (Bq/g) | Date A.D. | Error of age (± s.d.) |
|---|---|---|---|---|---|
| 0.5 | 0.359 | 0.334 | 0.013 | 1994 | 1 |
| 1.5 | 0.218 | 0.193 | 0.007 | 1984 | 3 |
| 2.5 | 0.172 | 0.147 | 0.001 | 1974 | 4 |
| 4.5 | 0.102 | 0.077 | 0.003 | 1954 | 8 |
| 6.5 | 0.073 | 0.048 | 0.002 | 1934 | 11 |
| 8.5 | 0.048 | 0.023 | 0.001 | 1914 | 15 |
| 12.5 | 0.029 | 0.004 | 0.000 | 1874 | 21 |
| 16.5 | 0.026 | 0.001 | 0.000 | 1833 | 28 |
| 20.5 | 0.026 | 0.001 | 0.000 | 1793 | 35 |
| 24.5 | 0.025 | 0.000 | 0.000 | 1733 | 42 |

**Table 2:** Summary of total $^{137}Cs$ activity in core QING6.

| Depth (cm) | $^{137}Cs$ Activity (Bq/g) | Error (Bq/g) |
|---|---|---|
| 0.75 | 0.085 | 0.004 |
| 1.25 | 0.100 | 0.005 |
| 2.25 | 0.042 | 0.006 |
| 3.25 | 0.035 | 0.004 |
| 4.25 | 0.025 | 0.005 |
| 5.25 | 0.014 | 0.004 |
| 6.25 | 0.000 | 0.000 |
| 7.25 | 0.000 | 0.000 |
| 8.25 | 0.000 | 0.000 |
| 10.25 | 0.000 | 0.000 |

**Table 3:** Radiocarbon dates from core QING6. Dates prefixed AA were analysed at the University of Arizona's NSF AMS Facility, USA, whereas those prefixed SUERC were analysed at the NERC Radiocarbon Laboratory at the Scottish Universities Environmental Research Centre, UK. All AMS $^{14}C$ ages were determined on bulk organic matter isolated from lake sediment samples by treatment with 5% HCl to remove all carbonate content before graphitization at the respective labs.

| Lab # | Depth (cm) | $\delta^{13}C$ | AMS $^{14}C$ age | Error | Corrected age | Median calendar age | 68.2% probability |
|---|---|---|---|---|---|---|---|
| AA69669 | 36.5 | -30.7 | 1405 | 50 | 747 | 689 | 665 – 725 |
| AA69670 | 47.5 | -27.9 | 1608 | 33 | 950 | 854 | 824 – 869 |
| AA69671 | 61.5 | -28.4 | 1596 | 33 | 938 | 852 | 798 – 871 |
| SUERC-1697 | 78.5 | -28.6 | 2199 | 33 | 1541 | 1440 | 1461 – 1514 |

**Table 4:** Modern and surface sediment AMS $^{14}C$ ages from Lake Qinghai. BO = bulk organic matter from surface sediments, AC = authigenic carbonate from surface sediments and DOC = dissolved organic carbon from modern lake water. Radiocarbon ages were combined using OxCal v. 4.0 (Bronk Ramsey 1995, 2001) and then calibrated using Bomb04NH2 (Hua & Barbetti, 2004).

| Lab # | Material | $\delta^{13}C$ | AMS $^{14}C$ age | Error | Median calendar age | 68.2% probability |
|---|---|---|---|---|---|---|
| AA69680 | BO | -25.4 | 640 | 32 | | |
| AA69679 | AC | -30.6 | 672 | 32 | 658 | 639 – 677 |
| AA57409 | DOC | -23.7 | 661 | 32 | | |

**List of figures**

**Figure 1 –** Location of Lake Qinghai on the northeastern Tibetan Plateau with predominant air masses. Numbers represent palaeoclimate archives discussed in text: 1 = Wanxiang Cave; 2 = Longxi, NE Tibetan Plateau; 3 = Dongge Cave.

**Figure 2 –** Unsupported $^{210}Pb$ activity (background=0.026 Bq/g), and total $^{137}Cs$ activity in Bq/g. The age model is a log-linear regression (simple model).

**Figure 3 –** Estimation of the OCE following the routine of Shen et al. (2005). The linear regression intercepts the modern-day at 737 $^{14}C$ yr BP. All dates are uncalibrated and not treated with any OCE offset.

**Figure 4 –** Mixed-effect regression age models (Heegaard et al., 2005) developed for QING6 based on median calendar ages. Plots A and B represent age models developed using all AMS $^{14}C$ dates, employing a constant and mu variance (k=5). Plots C and D represent age models developed based on the exclusion of the AMS $^{14}C$ date at 61 – 62 cm, employing a constant and mu variance (k=5). Constant variance employs a normal distribution, while mu variance is a function of the expected mean (Poisson-like distribution) (Heegaard et al., 2005).

**Figure 5 –** Age-depth model for QING6. Grey circles show corrected calibrated dates that were included in the mixed-effect regression age model. Error bars indicate 1-σ ranges (68% confidence intervals) of calibrated $^{14}C$ ages. $\delta^{18}O_C$ record (QING6) in

comparison with a high-resolution temperature reconstruction for China (Yang *et al.,* 2002); drought/flood index (D/F) for the NE Tibetan Plateau (Tan et al., 2008) and $\delta^{18}O_S$ record from Wanxiang Cave (Zhang et al., 2008) (smoothed using a 5-point moving average function (black line), which is overlain the raw data (grey line)). Shaded grey areas represent the Medieval Warm Period (MWP); Little Ice Age (LIA) and Twentieth Century (TC).

**Figure 6 –** A bi-plot of the $\delta^{18}O$ and $\delta D$ composition of modern waters from the Lake Qinghai region. Grey circles = Lake Qinghai water. Black squares = river waters. Open squares = rain and groundwater. GMWL is defined as $\delta D = 8\delta^{18}O + 10$. The local evaporation line is $\delta D = 6.05\delta^{18}O - 2.70$ as defined by linear regression.

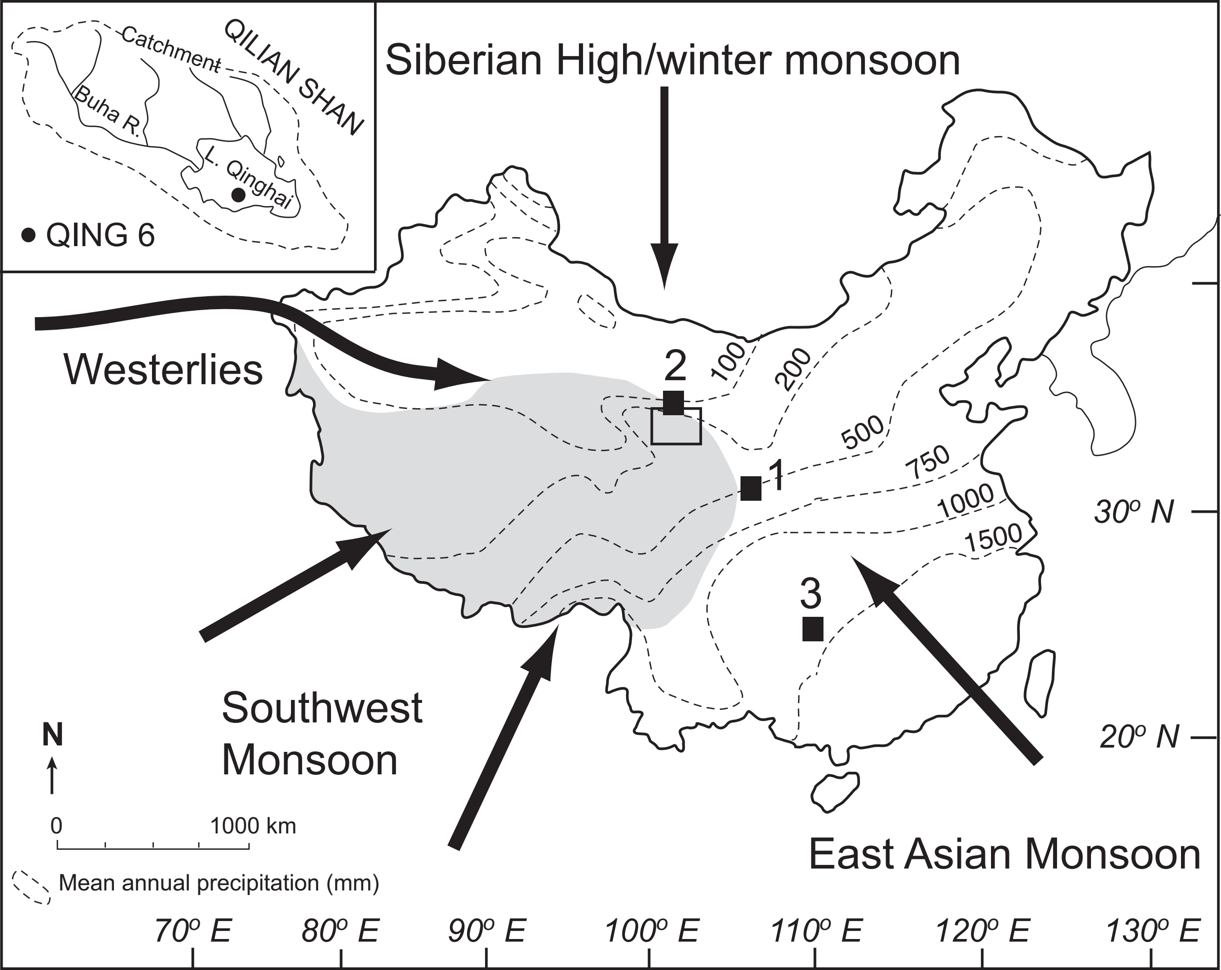

Catchment
QILIAN SHAN
Buha R.
L. Qinghai
QING 6
Siberian High/winter monsoon
Westerlies
2
100
200
500
1
750
1000
1500
3
30º N
20º N
Southwest
Monsoon
East Asian Monsoon
N
0
1000 km
Mean annual precipitation (mm)
70º E
80º E
90º E
100º E
110º E
120º E
130º E

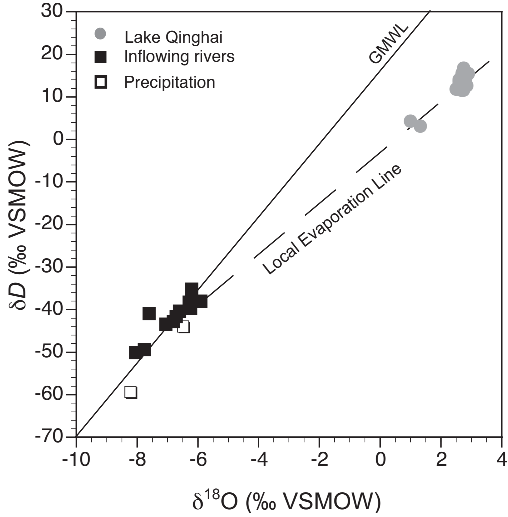

Lake Qinghai
Inflowing rivers
Precipitation
GMWL
Local Evaporation Line
30
20
10
0
-10
-20
-30
-40
-50
-60
-70
-10
-8
-6
-4
-2
0
2
4
δD (‰ VSMOW)
δ18O (‰ VSMOW)

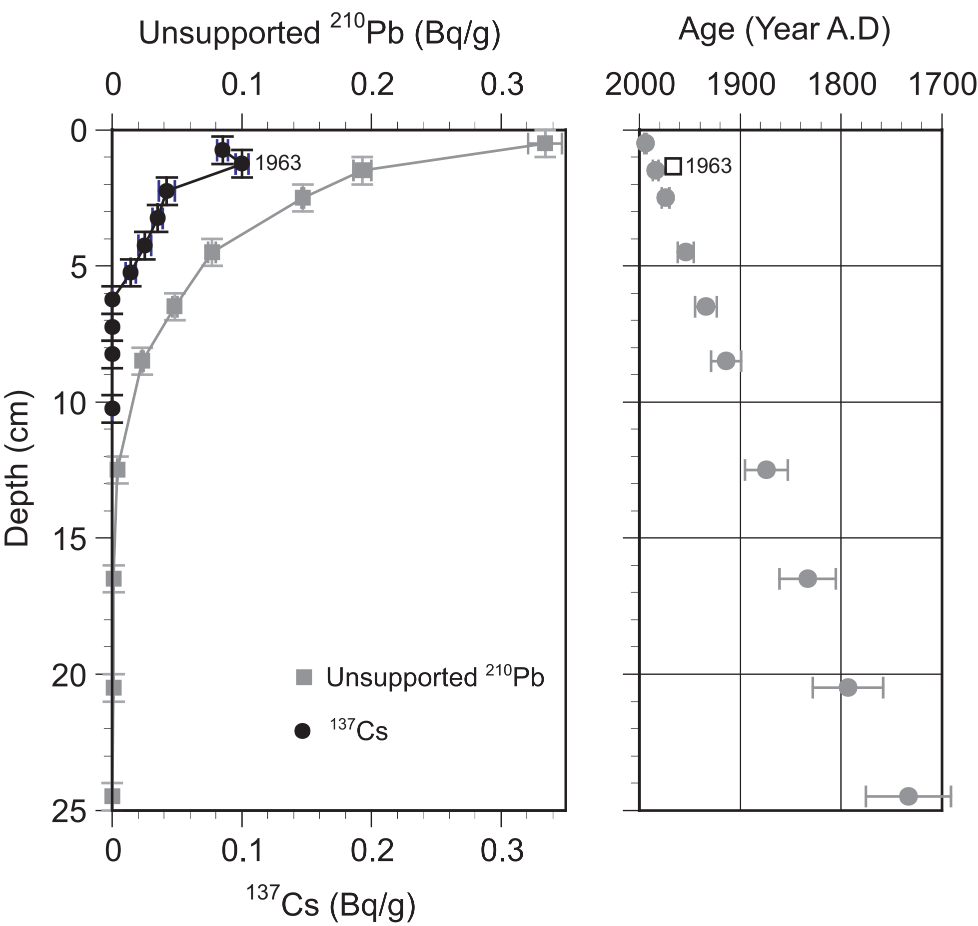

Unsupported $^{210}$Pb (Bq/g)
0
0.1
0.2
0.3
Depth (cm)
0
5
10
15
20
25
1963
Unsupported $^{210}$Pb
$^{137}$Cs
$^{137}$Cs (Bq/g)
Age (Year A.D)
2000
1900
1800
1700
1963

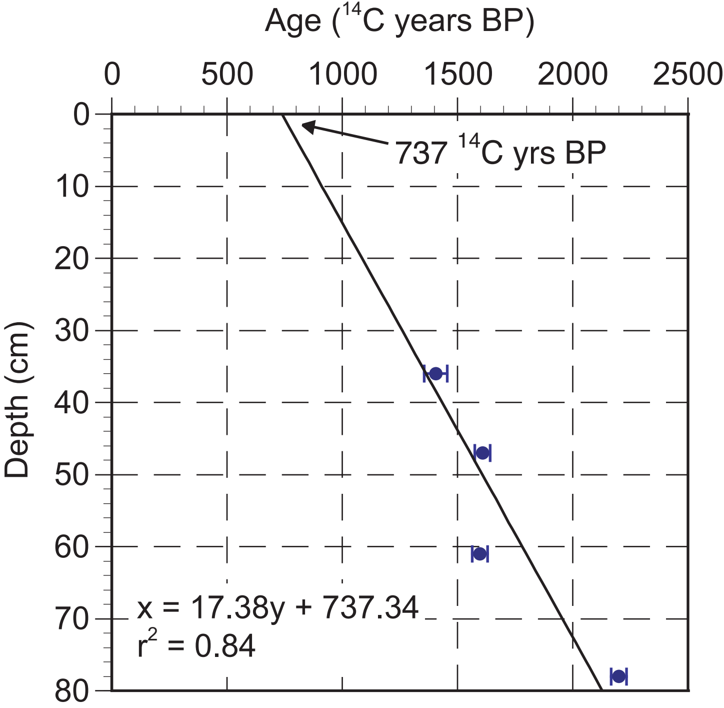

Age (14C years BP)
0
500
1000
1500
2000
2500
Depth (cm)
0
10
20
30
40
50
60
70
80
737 14C yrs BP
x = 17.38y + 737.34
r2 = 0.84

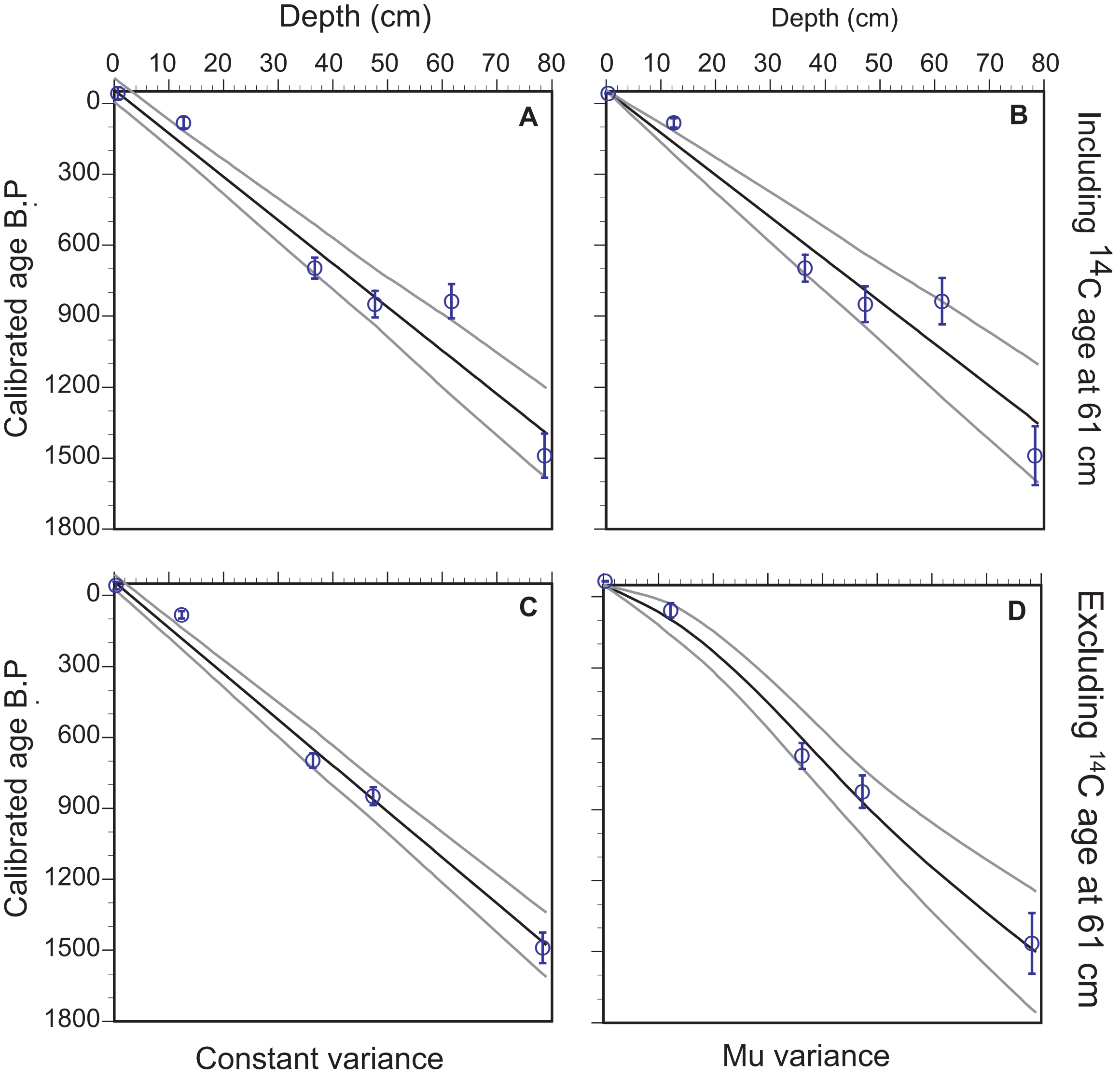
Depth (cm)
Depth (cm)
0
10
20
30
40
50
60
70
80
Calibrated age B.P.
0
300
600
900
1200
1500
1800
A
B
C
D
Including $^{14}C$ age at 61 cm
Excluding $^{14}C$ age at 61 cm
Constant variance
Mu variance

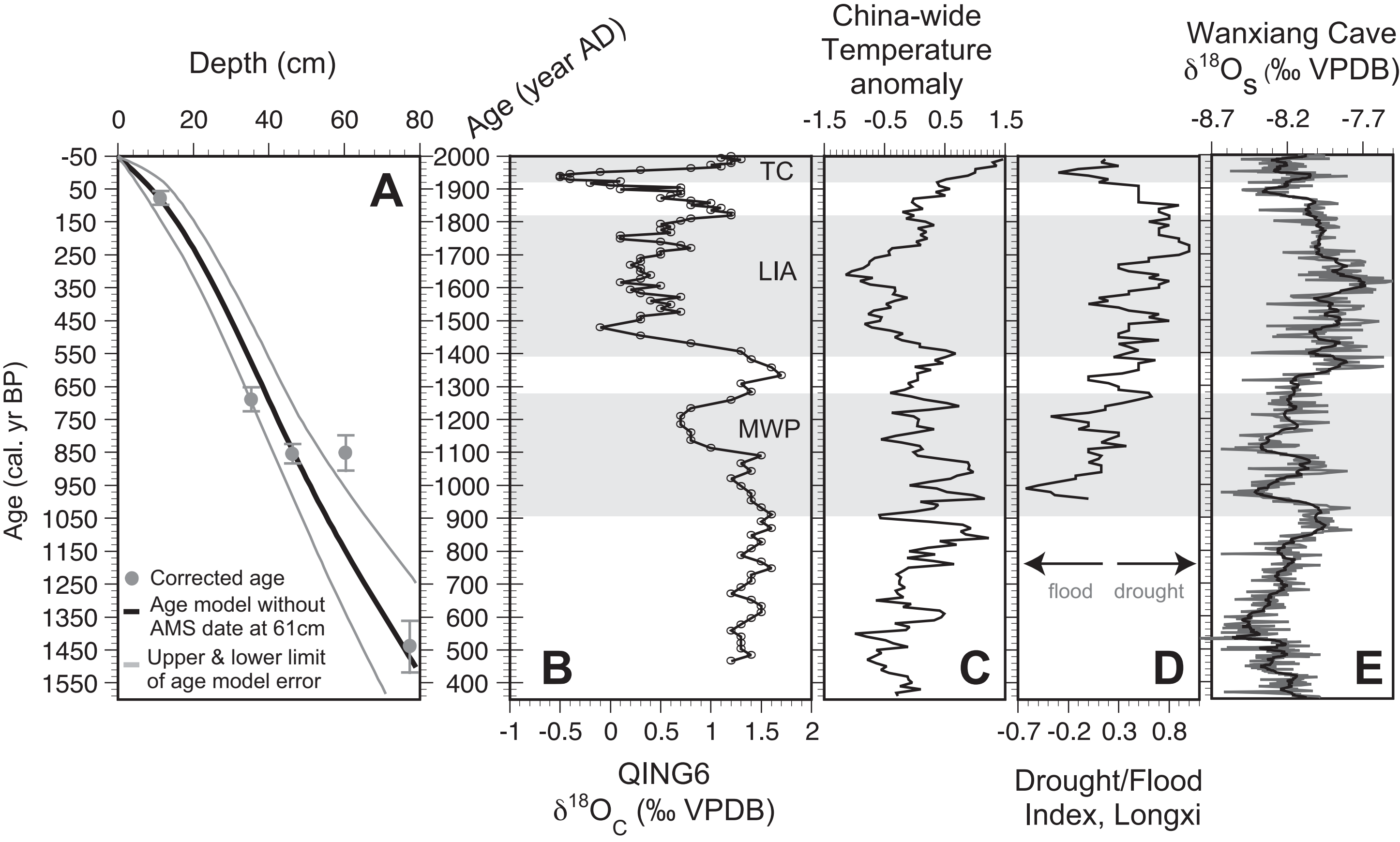

Depth (cm)
0 20 40 60 80
Age (cal. yr BP)
-50 50 150 250 350 450 550 650 750 850 950 1050 1150 1250 1350 1450 1550
A
Corrected age
Age model without AMS date at 61cm
Upper & lower limit of age model error
Age (year AD)
2000 1900 1800 1700 1600 1500 1400 1300 1200 1100 1000 900 800 700 600 500 400
TC
LIA
MWP
B
-1 -0.5 0 0.5 1 1.5 2
QING6
δ18OC (‰ VPDB)
China-wide Temperature anomaly
-1.5 -0.5 0.5 1.5
C
D
flood
drought
-0.7 -0.2 0.3 0.8
Drought/Flood Index, Longxi
Wanxiang Cave
δ18OS (‰ VPDB)
-8.7 -8.2 -7.7
E